

MOUNTAIN-PLAINS CONSORTIUM

MPC 18-349 | C. Liu, M. Zlatkovic, R. Porter, K. Fayyaz and S. Yu

Improving Efficiency and Reliability of Bus Rapid Transit



A University Transportation Center sponsored by the U.S. Department of Transportation serving the Mountain-Plains Region. Consortium members:

Colorado State University
North Dakota State University
South Dakota State University

University of Colorado Denver
University of Denver
University of Utah

Utah State University
University of Wyoming

Improving Efficiency and Reliability of Bus Rapid Transit

Xiaoyue Cathy Liu, Ph.D., P.E.
Assistant Professor
Department of Civil and Environmental Engineering
University of Utah
Salt Lake City, Utah, 84112
Phone: (801) 587-8858
Email: cathy.liu@utah.edu

Milan Zlatkovic, Ph.D., P.E.
Assistant Professor
Department of Civil & Architectural Engineering
Laramie, WY 82071
mzlatkov@uwyo.edu

Richard J. Porter, Ph.D., P.E.
VHB, Inc.
940 Main Campus Drive, Suite 500
Raleigh, NC 27606
rporter@vhb.com

Kiavash Fayyaz, Ph.D.
RSG, Inc.
307 W 200 S, Suite 2004
Salt Lake City, UT 84101
kiavash.fayyaz@rsginc.com

Song Yu
Department of Civil and Environmental Engineering
University of Utah
Salt Lake City, Utah, 84112

June 2018

Acknowledgements

The authors acknowledge the Mountain-Plain Consortium (MPC) and the Utah Transit Authority (UTA) for funding this research, and the following individuals from UTA on the Technical Advisory Committee for helping to guide the research:

- James McNulty
- Hal Johnson
- Jaime White
- Christopher Chesnut
- James Wadley

Disclaimer

The contents of this report reflect the views of the authors, who are responsible for the facts and the accuracy of the information presented. This document is disseminated under the sponsorship of the Department of Transportation, University Transportation Centers Program, in the interest of information exchange. The U.S. Government assumes no liability for the contents or use thereof.

ABSTRACT

In recent years, Bus Rapid Transit (BRT) systems have been gaining increasing popularity because of their effectiveness in improving urban mobility. The Utah Transit Authority (UTA) is the primary public transit provider in Salt Lake City and has implemented a 10.8-mile BRT route along 3500/3300 South in Salt Lake City. A total of 106 miles of BRT lines are planned throughout Utah, to be implemented by 2030, in an effort to alleviate congestion and increase ridership along major corridors. This research aims to utilize a modeling and simulation approach to help improve the efficiency and reliability of the high-capacity service, which makes BRT an appealing system for potential riders. First, a microscopic simulation is created to test a series of GPS-based transit signal priority (TSP) scenarios and evaluate their impact on transit and traffic operations. Second, a data-driven optimization method is implemented to understand the contributing factors of BRT dwell time and the benefits of an off-board fare collection system.

TABLE OF CONTENTS

1. INTRODUCTION	1
1.1 Background.....	1
1.2 Objectives	2
1.3 Outline of Report	2
2. LITERATURE REVIEWS	3
2.1 TSP.....	3
2.2 DT Modeling.....	4
3. STUDY NETWORK AND DATA COLLECTION	7
4. RESEARCH METHODOLOGY	9
4.1 Microscopic Simulation for TSP Analysis.....	9
4.1.1 Network, Control, Traffic, and Transit Inputs.....	9
4.1.2 Calibration and Validation	10
4.1.3 Transit Signal Priority	11
4.1.4 Simulation Scenarios.....	12
4.2 DT Modeling.....	12
4.2.1 Genetic Algorithm (GA) for Determining Behavior-Controlled DT	12
4.2.2 DT Modeling and Fare Payment Structure Analysis.....	14
5. RESULTS AND DISCUSSION	17
5.1 TSP Microscopic Simulation	17
5.1.1 Transit Travel Time.....	17
5.1.2 Non-transit Travel Time	19
5.1.3 Impacts on Side-Street Traffic.....	20
5.1.4 Network Performance.....	22
5.2 Results of DT Modeling and Fare Payment Structure Analysis	23
5.2.1 Result Interpretation	25
5.2.2 Testing Model Validity.....	27
6. CONCLUSIONS	29
6.1 TSP Performance Assessment vs. Microscopic Simulation	29
6.2 DT Modeling for TVM Effectiveness Analysis.....	30
REFERENCES	32

LIST OF TABLES

Table 2.1	Minneapolis, San Mateo, and Tampa TSP Evaluations	3
Table 2.2	Selection of Previous Studies on DT Modeling	5
Table 4.1	Simulation Scenarios	12
Table 4.2	Summary Statistics of Boarding Controlled (BC) Observations.....	14
Table 5.1	Total Transit Delays for 2-hour Simulation	19
Table 5.2	Total Side-Street Traffic Delays for 2-hour Simulation.....	21
Table 5.3	Transit and Non-transit Network Performances.....	23
Table 5.4	Optimal Model Specification with B-CTVM.....	24
Table 5.5	Summary Statistics of B-Cash and B-TVM	24
Table 5.6	Final Optimal Model Specifications with B-TVM and B-Cash	25
Table 5.7	Estimation Error Impact on B-TVM and B-Cash Coefficients	28

LIST OF FIGURES

Figure 3.1	BRT 35M Route Layout (source: www.rideuta.com)	8
Figure 4.1	Study Corridor.....	10
Figure 4.2	Results of (a) Calibration and (b) Validation (veh=number of vehicles).....	11
Figure 5.1	Transit Travel Times: (a) Eastbound and (b) Westbound (W = west; E = east).	18
Figure 5.2	Non-transit Travel Time: (a) Eastbound and (b) Westbound.....	20
Figure 5.3	Data for Side-Streets: (a) Average Queue Lengths and (b) Average Number of Stops per Vehicle	22

EXECUTIVE SUMMARY

Bus Rapid Transit (BRT) is an innovative, high-capacity, lower-cost public transit solution that can significantly improve mobility. It is usually defined as an integrated system with a strong, transit-oriented identity, which consists of running ways (very often exclusive lanes), specially designed rail-like stations, high-capacity low-floor vehicles, improved services, and state-of-the-art Intelligent Transportation Systems (ITS). It provides similar quality of service as rail transit at much lower construction and operational costs to the transit organization, and retains the flexibility of buses. BRT has the potential to significantly improve efficiency and reliability of public transit, which leads to an increase in ridership. Certain *operational strategies* significantly help BRT in improving travel times, speeds, and headway adherence, with the most beneficial seen from the implementation of Transit Signal Priority (TSP) and off-board fare collection. ITS technologies, such as GPS tracking devices, Automated Passenger Counters (APC), Ticket Vending Machines (TVM), advanced detection systems, and signal performance monitoring systems, are now widely used by transit and state DOT agencies. These systems, by providing performance-related data, can be used to further improve the efficiency and reliability of these BRT systems. This research will focus on the evaluation and analysis of two operational strategies for improving the efficiency and reliability of BRT system: TSP and fare collection methods. The study reviews different TSP systems (conventional detection vs. GPS, conditional active TSP considering ridership and schedule/headway adherence, and adaptive TSP considering a wide range of traffic and transit operations), and fare collection methods being used (prepaid, tickets sold by the driver, off-board TVMs, on-board TVMs), and quantitative analysis is performed based on field and simulated data to evaluate the effectiveness of various strategies. The study is built upon the Utah Transit Authority (UTA) BRT system; however, the research result is quite transferable to other BRTs in the metropolitan areas with similar system designs and can serve as a reference for transit planners and engineers on the national level.

1. INTRODUCTION

1.1 Background

The Utah Transit Authority (UTA) is the primary public transit provider in Salt Lake, Utah, counties of Davis, Weber, Box Elder and Tooele. The UTA's system consists of a commuter rail (FrontRunner), light rail transit (LRT - TRAX), bus rapid transit (BRT - MAX), streetcar, bus (local, express, special purpose), and paratransit modes. In recent years, BRT systems have been gaining increasing popularity due to their effectiveness in improving urban mobility. BRT provides low-cost, reliable, and comfortable transit solutions that offer great potential to meet increasing transit demand. The relatively shorter construction cycle, competitive operating cost, increased capacity, and flexible integration into community are all the appealing traits for BRT implementation. Currently, there is one BRT deployment, 35MAX BRT, that operates on 3300S-3500S corridors between Millcreek and Magna in Utah, with several lines planned for the near future (5600 West, Provo/Orem, 4700 South, 3300 South, and others) Many of the delays associated with regular transit systems are minimized through the implementation of BRT mainly with the provision of dedicated bus lanes to avoid mix traffic congestion, off-board fare collection, transit signal priority (TSP), just to name a few.

TSP is an operational strategy that facilitates the movement of in-service transit vehicles through intersections controlled by traffic signals (Smith et al., 2005). It is typically achieved by extending the green or reducing the red phase for transit vehicles and is intended to result in shorter and more reliable travel times and improved schedule adherence. Prior TSP deployments in the United States generally indicated average bus travel time savings of between 2% and 20%, with 8% to 12% as the most typical range (TCRP, 2007). However, minor increases in the delay of side-street traffic are expected with TSP implementations (Smith et al., 2005; TCRP, 2007). GPS-based TSP uses a GPS to achieve real-time bus locating and advanced wireless communication technologies to achieve comprehensive analysis of operating information. GPS-based TSP has advantages, including low infrastructure costs, flexibility in detection distance, and ability to transmit large amounts of data (Li, et al., 2008). GPS-based TSP can offer conditional signal priority, which considers multiple constraints, such as transit vehicle occupancy, schedule adherence, and real-time traffic conditions, before granting signal priority to transit vehicles. Thus, signal priorities are provided more efficiently and on a more informed basis, with fewer impacts on other traffic operations than the use of unconditional TSP. With its advantages, GPS-based TSP is being considered in many U.S. cities. However, existing field implementations of GPS-based TSP are rare, because the technologies are relatively new and its benefits and impacts have not been fully evaluated.

Meanwhile, transit service reliability and efficiency are influenced by the variability in bus operating times. Bus operating time consists of two main components: (a) time spent between stops (running time) and (b) time spent at stops [dwell time (DT)]. Variability in these components can result in an increase in transit headway variation and, consequently, a worsening experience for transit users because of inconsistent wait times. The DT can account for a significant portion of the bus operating time (Tirachini, 2013). Therefore, understanding the nature of factors influencing DT will assist transit authorities with planning and operating their bus systems more effectively. UTA guidelines suggest off-board fare collection be used on all BRT lines (UTA, 2014). A total of 106 miles of BRT lines are planned throughout Utah, to be implemented by 2030, in an effort to alleviate congestion and increase ridership along major corridors. Thus, a thorough understanding of the contributing factors for BRT DT and the benefits of off-board fare collection system is becoming particularly critical as additional BRT lines are in the planning phase.

1.2 Objectives

The overarching goal of this project is to assess the impacts of various strategies (i.e., TSP and off-board fare collection system) on the BRT's operational performance. The first objective is to evaluate the benefits and impacts of GPS-based TSP at the transit corridor level by using microscopic simulation. The test bed is the 3300 South corridor in Salt Lake County, Utah. A proposal was introduced to convert UTA Bus Route 33 running along the corridor into a mixed-traffic BRT line. Eight simulation models are created to cover different combinations of transit operation patterns and TSP strategies. Outcomes are compared and analyzed to determine the relative changes in benefits and impacts on transit and non-transit traffic operations resulting from GPS-based TSP compared with other TSP strategies in both regular and rapid transit operation patterns.

The second objective of this study is to quantify the magnitude of advantages of off-board fare collection system along the existing 35M BRT line. This is achieved by determining the contributing factors of DT. This requires fare payment structure analysis, which could be challenging due to the non-electronic fare media that do not have electronic footage. We propose a genetic algorithm-based optimization method and regression model to disaggregate the individual contributions to DT of fare payment options, station placement, design, and the built environment. The modeling approach is transferable to any transit route or system equipped with automatic passenger counters. The fare payment analysis can assist transit agencies with service optimization and performance assessments.

1.3 Outline of Report

The rest of the report is structured as follows. Section 2 summarizes literature on TSP and DT modeling efforts. Section 3 describes the data collection process. Section 4 presents the methodology for both the TSP microscopic simulation setup and the DT modeling and fare payment structure analysis. Section 5 demonstrates the results using UTA's transit corridor. Section 6 presents the conclusion of this study and recommendations for future research.

2. LITERATURE REVIEWS

2.1 TSP

Previous evaluations of TSP corridors showed several benefits of TSP implementations. TSP projects in Portland, Oregon, along Powell Boulevard and Tualatin Valley Highway that used early green–green extension strategies brought, respectively, reductions of 5% to 8% and 1.4% to 6.4% in bus travel times. The Cermak Road Bus Priority Project in Chicago, Illinois, compared situations with and without TSP on the basis of optimized timings and showed a 6.8% reduction in bus travel times and a 43.8% reduction in bus signal delays with TSP. A study of Rainier Avenue TSP in King County, Washington, reported a reduction in transit travel time of 8%, a reduction in transit signal delays of 24% to 34%, and a change in person delays at intersections of –17% to +12% (Innovative Transportation Concepts, Inc., 2001). Benefits of TSP vary significantly from site to site. Therefore, new TSP strategies should be evaluated before implementation (Park and Hu, 2014). Field studies are performed throughout the implementation process, but simulations are able to evaluate TSP systems before their deployments. Most recent studies have used simulations to evaluate TSP benefits and impacts. Field studies, however, still play a key role, particularly with respect to collecting data for validations of simulation models (Dale et al., 1999). INTEGRATION microsimulation has been used by Dion et al. (2004) and Dion and Rakha (2005) to evaluate TSP along transit corridors with different types of signals. VISSIM microsimulation was applied by Chen et al. (2008), Ghanim et al. (2013), and Zlatkovic et al. (2013) in their evaluations of TSP on, respectively, a BRT corridor in Beijing, a bus corridor on the campus of Michigan State University in East Lansing, Michigan, and a BRT corridor in Salt Lake County. Additional example applications of other simulation tools, such as CORSIM (Bloomberg and Dale, 2000) and Aimsun (Liao and Davis, 2011) also exist. A limited number of studies have been conducted to evaluate GPS-based TSP in the United States at a corridor level. Three studies identified for this literature review are the Central Avenue TSP evaluation by Liao and Davis (2011) in Minneapolis, Minnesota; the SamTrans Route 390–391 adaptive TSP study by Li et al. (2010) in San Mateo, California; and the Hillsborough Area Regional Transit BRT corridor TSP study by Martin et al. (2010) in Tampa, Florida. Evaluation results from the three studies are summarized in Table 2.1. All three projects proved through field tests or microscopic simulation to provide in benefits in reductions of transit delays and increases in average travel speed, with insignificant impacts to other traffic operations.

Table 2.1 Minneapolis, San Mateo, and Tampa TSP Evaluations

Location	TSP Type	Evaluation Method	Measurement	Result (before and after TSP) (%)
Minneapolis	GPS + wireless communications	Field test	Measured travel time	Northbound: –6 Southbound: –4
			Schedule travel time	Northbound: –13 Southbound: –5
San Mateo	Adaptive TSP (centralized GPS)	Field test	Intersection delay	Northbound: –18.5 Southbound: –32
			Stops on reds	Northbound: –9.5 Southbound: –10.8
			Average waiting time per stop	Northbound: –10.5 Southbound: –18.5
			Travel time (excluding dwell time)	Northbound: –7.3 Southbound: –10.4
			Average trip running speed	Northbound: +4.9 Southbound: +5.6
Tampa	GPS + optical communications	Microscopic simulation	BRT travel time	Northbound: –5.7 Southbound: –5.4
			BRT average speed	Northbound: +6.0 Southbound: +5.7

2.2 DT Modeling

The Transit Capacity and Quality of Service Manual (TCQSM) defines DT as the sum of passenger service time, boarding lost time, and door opening and closing time (TCRP, 2003). Passenger service time is understood to be the biggest contributor to DT. It is influenced by passenger demand, fare payments, vehicle configuration, passenger load, door usage, and platform configuration (TCRP, 2003). There are also secondary factors influencing DT to various extents, such as atypical passenger boarding, passenger age, time of the day, and fare payment issues (Tirachini, 2013). The effort to identify factors affecting transit DT has led to a wide-scale use of linear regression analysis since the 1970s (Feder, 1973; Guenther, 1983; Levine and Torng, 1994; Bertini and El-Geneidy, 2004). DT modeling in this way, similar to any statistical or econometric model, relies on a sample of data gathered via different sources to estimate model parameters. Manual data collection provides detailed and accurate data, yet typically involves labor-intensive ride checks. As a result, project budgets and time constraints usually limit the sample sizes. Recent years have seen the growing adoption by transit agencies of technologies such as automatic passenger counter (APC), automatic vehicle location (AVL), and automatic fare counting (AFC) systems, and researchers have started to use these data sources for DT modeling. Automatic data collection overcomes the main challenges faced by manually collected data, such as limited sample sizes due to time-intensive data collection, yet it also comes with downsides of its own related to resolution, accuracy, and fragmented data. For example, the impacts on DT on fare transactions that do not have electronic footage have not been studied in previous work that used automatically collected data because of the absence of such information. As one of the major factors influencing passenger service time, fare payment structure has a direct impact on DT. Previous studies have shown that passengers' boarding and alighting times depend on their fare payment method, and these findings are captured in the TCQSM methodologies, which include individual passenger service times by fare payment method (TCRP, 2003). APC data provide the total number of passengers boarding and alighting at each station, while AFC data provide separate counts of smart card users. However, other payment options, including prepaid passes or cash transactions, cannot be traced from the APC/AFC dataset, resulting in the need for new analysis methods that can quantitatively identify the impact of each separately.

The classic linear regression model with ordinary least squares (OLS) estimation has been widely used as the means for modeling bus DT. Previous studies have investigated a broad range of DT model specifications, from simple to multivariate regression analysis. In the simple DT models, DT is considered solely a function of the number of boarding and alighting passengers (Levinson, 1983). In multivariate DT models, several different factors are considered, such as fare payment methods, crowding effect, and passenger population. It is usually expressed in the format similar to that of Tirachini (2013):

$$DT = \sum_{i=0}^N \alpha_i * B_i + \sum_{j=1}^2 \beta_j * A_j + C \quad (1)$$

where α_i is the average boarding time per passenger using the i^{th} fare payment method; B_i is the corresponding amount of boarding passengers; N is the number of available fare payment methods; β_j is the average alighting time per passenger using the j^{th} door; A_j is the number of alighting passengers through the j^{th} door; and C is time spent for door opening and closing (dead-time). The multivariate models are likely a more realistic representation of a DT model, especially given the dynamics of passenger boarding and alighting.

A summary of a selected number of studies on DT modeling is shown in Table 2.2. A fare payment method was repeatedly shown in the literature to be a major influence on DT. Kraft and Bergen (1974) were probably among the first to have studied such impacts. They found that on-board exact change fare payment was three seconds faster than on-board change-given fare payment. Guenthner and Hamat (1988) reported marginal variation of impact on DT from different fare payment methods. Fletcher and El-Geneidy (2013) determined that on-board cash fare payers had two seconds slower boarding times than prepaid pass holders. Tirachini (2013) reported that DT per passenger boarding paying with cash exact fare was seven seconds less than passengers paying with cash change-given. Milkovits (2008) analyzed the impact of fare payment methods and found that smart media cards were roughly 1.5 seconds faster to process than magnetic stripe tickets. Sun et al. (2014) used data from 3.3 million smart card transactions in Singapore and found that the boarding (alighting) interval per passenger using a smart card was about 1.9 (1.5) seconds. A closer review of these studies showed that the estimated impact of individual fare payment methods varied across routes and transit systems. For example, boarding time for magnetic strip fare payment method was estimated to be 4.8 seconds in the Milkovits (2008) study, but 5.5 seconds in Tirachini (2013). While these different estimates reveal possible variations on fare payment structure impact because of interactions with other key variables, or indicate potential omitted (confounding) variable issues, the data are conclusive in one important aspect: they reveal that different payment structures triggered changes in DT and that the impact of different payment methods was uncovered in study after study. In other words, fare payment strategies can be implemented to improve the reliability of transit operation by reducing DT magnitudes and variation.

Table 2.2 Selection of Previous Studies on DT Modeling

Author	Data Collection Method	Sample Size	Factors studied
Feder, 1973	Manual	N/A	Boarding and alighting
Kraft and Bergen, 1974	Manual	N/A	Time of day, fare payment method
Levinson, 1983	Manual	N/A	Boarding and alighting
Guenther and Hamat, 1988	Manual	266 passengers observed	Boarding and alighting, fare payment method
Lin and Wilson, 1992	Manual	N/A	Dwell time per door, Crowding effect
Ashtiani and Iravani, 2003	Manual	3,454	Number of doors used, boarding and alighting, crowding effect
Rajbhandari et al., 2003	APC/AVL	40,594	Boarding and alighting, crowding effect, time of day
Dueker et al., 2004	APC/AVL	350,000	Lift operation, time of day, crowding, schedule adherence Boarding and alighting
Milkovits, 2008	APC/AVL/AFC	173,750	Fare payment method, alighting through each door, crowding effect
Fletcher and El-Geneidy, 2013	Manual	1,746	Crowding effect, fare payment method
Tirachini, 2013	Manual	1,604	Crowding, passenger age, fare payment method
Stewart et al., 2014	APC/AVL	1,213,691	Boarding and alighting through each door, crowding effect, presence of traffic light, stop effect
Sun et al., 2014	AFC/APC	3,300,000	Smart card users time interval, crowding

The aforementioned studies on DT and fare payment methods can be categorized on the basis of data sources for model estimation purposes, usually by either manual or automatic data collection. While both face their own challenges and limitations in studying fare payment impacts, automatic data collection has steadily become a more promising option due to the mass amount of information that can be gathered and the cost effectiveness of doing so. Yet solely resorting to automatic data collection might, at times, downplay the significance of payment methods that do not have electronic footages, which are indeed still popular in a large number of transit systems, leaving their impact unknown or unjustified.

3. STUDY NETWORK AND DATA COLLECTION

UTA is the primary public transit provider in Salt Lake City, Utah, and in Davis, Weber, Box Elder, and Tooele Counties in Utah. The growth of economic development and opportunities necessitated mobility enhancements in these counties, especially via public transit in recent decades. The ambitious program of transit construction, led by UTA, has simultaneously spanned across light rail (LRT-TRAX), bus rapid transit (BRT-MAX), commuter rail (FrontRunner), streetcars, and buses (local, express, and special purpose) since the 1990s. Of all the transit options available, BRT offers a unique service by combining the flexibility of buses with the efficiency of rail. The 35M MAX BRT was the first BRT line in Salt Lake City, with UTA starting its operation in 2008. The bus runs a 10.8-mile distance on the 3300 S/3500 S corridor connecting the suburban town of Magna, Utah, and the light rail station at Millcreek.

Following in the footsteps of the 35M BRT pioneer project, several BRT lines are also being planned in the near future (5600 West, Provo–Orem, Utah, 4700 South, and 3300 South). The lessons learned and data gathered from 35M MAX can thus be directly applied for informed planning, design, and ultimately enhanced performance of these future projects. The 35M BRT uses low-floor, three-door buses that are 40 feet in length. The buses have 28 seats and 32 standees, for a total capacity of 60 passengers. The 35M BRT buses run on 15-minute headways on weekdays and 30-minute headways every Saturday. The buses use, on average, about 45% of their capacity during peak hours; thus, a crowding condition rarely occurs. Several fare payment options are available, including onboard cash payments with exact change into the fare box, electronic fare payments with a smart card, prepaid tickets purchased from a ticket vending machine (TVM), and transfer tickets. The 35M BRT drivers are instructed to use all doors for boarding and alighting, and no fare inspection is required; thus, some fare evasion is expected. All three doors are equipped with smart card readers (tap on and off), and only passengers who wish to use onboard cash payments are required to board at the front door. A TVM is located at every BRT station, and no fare validation on boarding is necessary. The direct benefit of TVMs is the reduction in DT and operational delays associated with collecting a fare and the resulting interaction between drivers and passengers. Thus, 35M BRT provided an excellent platform for DT and fare payment structure analysis, with the modeling results being potentially useful to inform the upcoming BRT project designs. Figure 3.1 shows the 35M MAX BRT route layout. The BRT line starts at the Millcreek Station and ends at the 3500 South 800 West Station. The Magna loop is not part of the BRT line; however, the same fleet is used to operate that segment. The 35M BRT line uses center-running dedicated lanes along 3500 South between 2810 West and 3600 West and runs in mixed traffic for the rest of the route (right-of-way C). There are 14 stations in each direction (totaling 28 stations).

To model DT and the fare payment structure quantitatively, stop-level data were needed. Data used in this study were collected through APC-AFC systems, with the use of sample manual checks for validation purposes. APC-AFC records were obtained for May 2014. The APC records included a total of 34,937 observations for 28 stops and provided information on travel direction, station ID and location, bus departure and arrival time, DT, number of boarding and alighting passengers, and station spacing at every station. AFC records included a total of 24,121 observations, with each entry representing individual passenger tap-on (boarding) or tap-off (alighting) at a specific date, time, and station. AFC and APC data were post-processed for matching on the basis of the following criteria: (a) AFC and APC records should have the same date and (b) the same station ID, and (c) the time stamp difference between the matching records is less than two minutes (to accommodate any measurement error). If AFC and APC data entries matched each other, then the AFC record was added to the corresponding APC observation. When an abnormal match appeared (e.g., AFC boarding greater than the total boarding), the record was removed from the data set. This process was completed with C++. Quality checks were also applied to the APC data set for sensor detection malfunction. A DT that was longer than three minutes or an average DT per passenger that was less than one second was considered an erroneous data record. To further validate the

automatic data collection and modeling results, a testing data set was collected to compare against the electronic data. Manual data collection was conducted on February 10, 2015, along 35M BRT during three peak periods (7 to 9 a.m., 11 a.m. to 1 p.m., and 4 to 6 p.m.). The data recorded consisted of 120 observations of the number of onboard cash payers and prepaid pass holders. In addition, 3,340 APC and 975 AFC records were gathered for that day, and the same matching process was conducted. The 120 manually collected observations were integrated into the APC-AFC database for model validation.

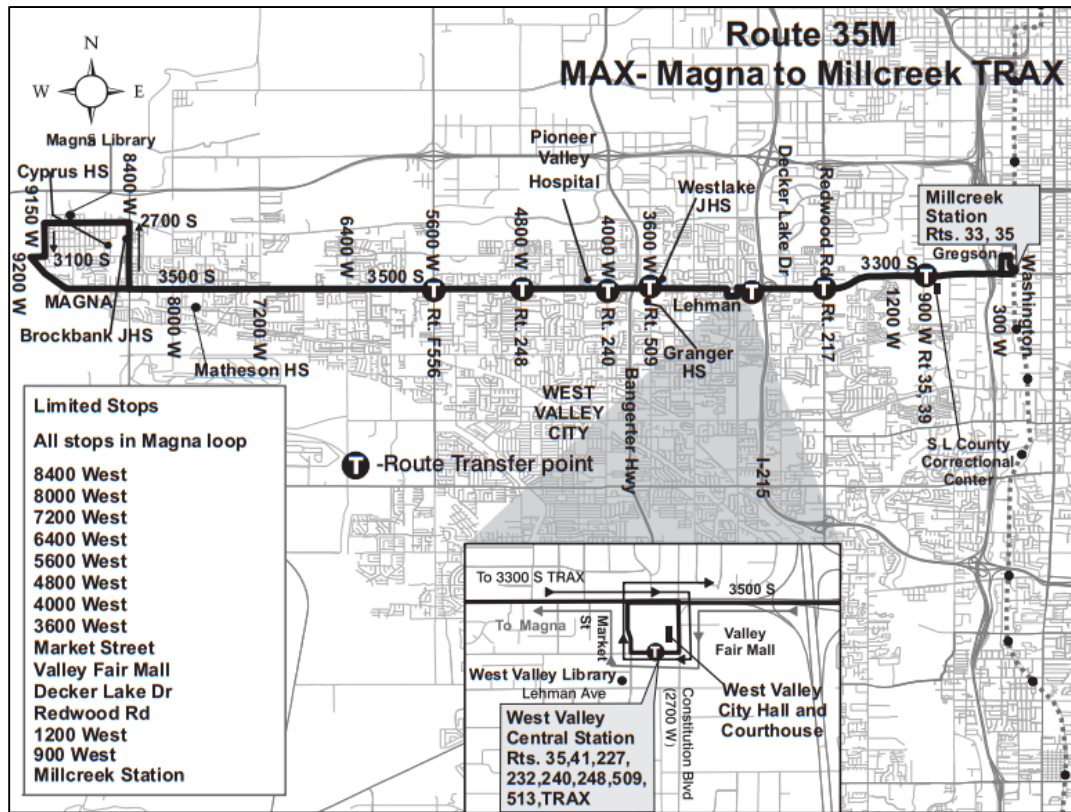


Figure 3.1 BRT 35M Route Layout (source: www.rideuta.com)

To facilitate TSP microscopic simulation, transit operation data were collected for Bus Route 33. The data set consisted of GPS and automatic passenger counter data from April 14 to August 16, 2014. Information in the data set included trip numbers, stop numbers and names, actual stopping time, schedule, traveled distance, dwell time, and passenger boardings and alightings. Data from trips during the Tuesday and Thursday afternoon peak periods (4 to 6 p.m.) were used to develop bus schedules, boarding numbers, and alighting percentages. Traffic data were obtained through the annual average daily traffic maps created by the Utah Department of Transportation (UDOT, 2015), Synchro models from UDOT, and field data collection. The UDOT annual average daily traffic map is a Google Earth .kmz file consisting of annual average daily traffic data from 2011 to 2013 for major urban and rural road sections in Utah. The Synchro models consisted of historical turning movement data for a few signalized intersections along the study corridor. Field data collection was performed to obtain turning movement data for key signalized intersections and segmental travel time data along the study corridor. Turning movement data were collected on the study corridor at State Street, Main Street, 700 East, and Highland Drive intersections in the fall of 2014 during weekday afternoon peak periods. Travel time data were collected along 3300 South (between West Temple and Highland Drive) in the fall of 2014 and spring of 2015 during the afternoon peak. The actual signal timing data for all signalized intersections along the study corridor were obtained in the UDOT traffic operations center.

4. RESEARCH METHODOLOGY

4.1 Microscopic Simulation for TSP Analysis

VISSIM was used for the network modeling in this research. VISSIM is a microscopic, time-step and behavior-based simulation platform of urban traffic and public transit operations. The modeling process was performed in VISSIM Version 5.40. The existing network was modeled, calibrated, and validated by using field data from the study corridor, including network geometry, traffic, and transit operations. VISSIM's features for transit operations enabled the modeling of basic transit parameters, including routes, transit stops, time scheduling, TSP, and passenger movements. Passenger movements consisted of passenger arrivals at stops that were based on a Poisson distribution, passenger boarding for each stop, and passenger alighting that was based on a user-defined alighting percentage for each stop. The GPS-based TSP tool was modeled by applying the functionality of the component object model of VISSIM interfacing with Excel Visual Basic for Applications programming. The final output from this process was a validated and calibrated simulation model of the existing conditions of the study corridor for the afternoon peak period, with a 15-minute warm-up time. The same model was later used for evaluating seven TSP and BRT scenarios. All VISSIM simulations for these scenarios were run for five random seeds, and all results represented averaged values from five measurements.

4.1.1 Network, Control, Traffic, and Transit Inputs

The study corridor was 3300 South, an urban principal arterial in Salt Lake County. UTA Bus Route 33 runs along 3300 South and Wasatch Boulevard, with a 1-mi loop around Millcreek TRAX (light-rail) Station at the west end of the corridor, as shown in Figure 4.1. The 2.3-mile study section between West Temple and Highland Drive (dark, solid line in bottom half of Figure 4.1) has 11 signalized intersections and is the higher-volume section of the 3300 South corridor with more commercial land use. As the eastern section of the corridor has a higher percentage of residential land use in adjacent areas, with significantly lower traffic volumes, it was not analyzed. The simulation network was constructed to follow the actual layout obtained from Google Earth and field observations. The desired speeds were set as cumulative distributions, with the actual speed limits as 85th-percentile speeds. The speed limit along the study section is 35 mph. Traffic signals were set according to the UDOT's design guidelines for signalized intersection and field timing data for signals by using ring barrier controllers in VISSIM. The hourly traffic volumes at the east and west ends of the study section, as well as at the side streets, were calculated by using 2013 annual average daily traffic data. Turning movements were set on the basis of Synchro models and field data. Traffic was generated and distributed on the network by using static assignment. Bus routes were modeled according to actual transit operation data. The modeling included defining the route, bus stop locations, schedule, passenger boardings (in counts), and passenger alightings (in percentages of passenger loads).

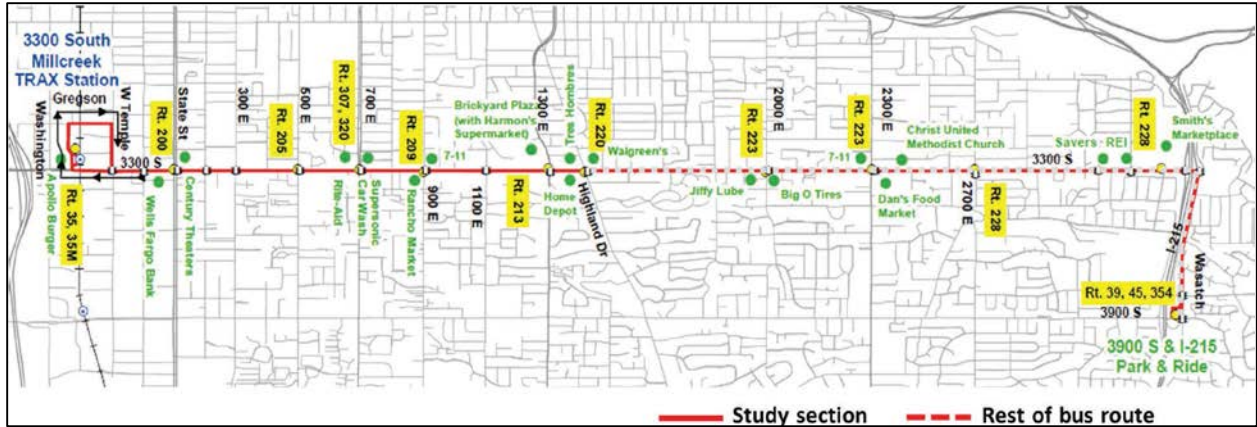


Figure 4.1 Study Corridor

UTA Bus Route 33 runs in mixed traffic along the 3300 South Corridor on a 15-minute headway during afternoon peak hours. The study section has one bus terminal (Millcreek TRAX Station), 17 eastbound bus stops, and 16 westbound bus stops. The average eastbound running time of Route 33 from Millcreek Station to Highland Drive was 15 minutes during afternoon peak, while the average westbound running time along the same section was 12 minutes. The average dwell time at eastbound stops within the study section was seven seconds, while for westbound stops it was eight seconds. The average occupancy of eastbound buses within the study section was 27 passengers, while for westbound buses it was 18 passengers. The schedule reliability of Bus Route 33 during the afternoon peak, defined by the percentage of on-time (with a late allowance of 0 to 4 minutes) arrivals at stops, was 90.9% for eastbound and 94.2% for westbound trips. For the BRT scenarios, the 15-minute headway and mixed-traffic right-of-way were kept in the simulation. The numbers of bus stops were reduced to seven for the eastbound direction and five for the westbound direction, keeping a 0.3- to 0.5-mile spacing with far side and midblock settings. Queue jump lanes were provided at higher-volume intersections, including State Street, 700 East, and 1300 East. BRT vehicles were provided with a separate, short (three-second) early-green signal to move into the bus loading area at the far side of the intersection, ahead of other through traffic (Zlatkovic et al., 2013).

4.1.2 Calibration and Validation

The existing network model was calibrated and validated on the basis of field data. Calibration was performed on the basis of traffic movement counts at major signalized intersections of the corridor. Segmental travel times between each pair of signalized intersections were used for validation. Simulation outputs were compared with field data by means of the charts shown in Figure 4.2. For both the calibration check of turning movements and validation check of travel times, the R^2 -values (.9972 and .8552, respectively) implied that the existing network simulation model closely matched the observed data and accurately reflected real-world situations.

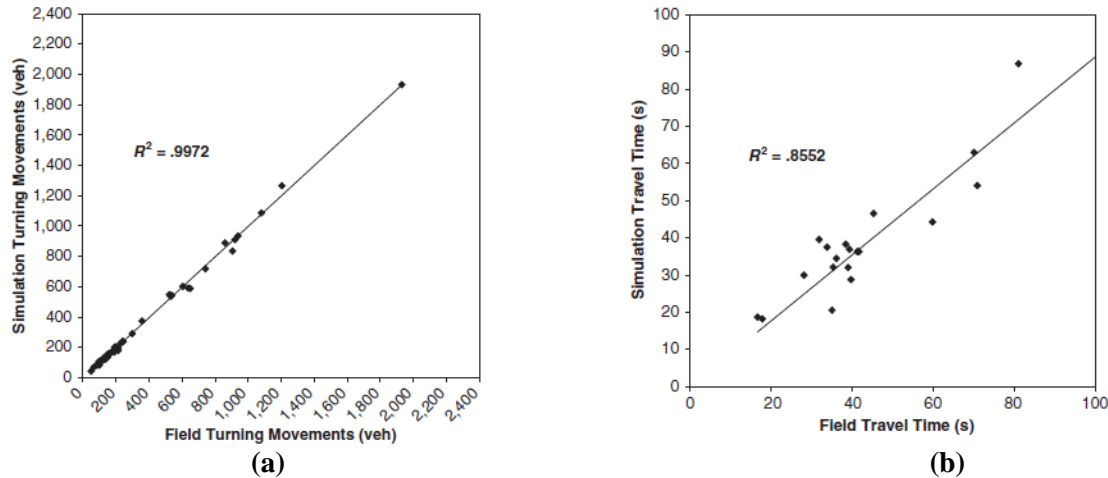


Figure 4.2 Results of (a) Calibration and (b) Validation (veh=number of vehicles)

4.1.3 Transit Signal Priority

The VISSIM ring barrier controllers for traffic signals have built-in TSP modules. The TSP strategy was enabled in signal controllers of all 11 signalized intersections along the 3300 South study section. Green extension–early green strategies were used for the TSP. The maximum-green extension–early green provided in the model was 10 seconds, which is the current TSP setting used by UDOT and UTA on BRT routes. In actual implementation, traditional TSP applies fixed or distance-limited detections, such as inductive loops–transponders or infrared beacons (Chang, 2012). In the simulation models, traditional TSP was achieved by using dedicated detectors installed before traffic signals along the transit corridor. In this study, the TSP detection distance was set to 500 feet.

GPS units installed on buses can locate vehicle positions and record time, and GPS-based TSP uses these inputs to achieve flexible granting of signal priority. In this study, the GPS-based TSP was modeled with the VISSIM interface for the component object model and Excel Visual Basic for Application programming. The program checked the buses’ position in the network and activated TSP when the bus reached a preset activation zone (a certain distance before signals). The length of activation zones can be preset flexibly. In this study, the length was set to 500 feet before signals for direct comparison with traditional TSP outcomes. Conditional TSP (CTSP) tools can be achieved by expanding the constraints for granting of signal priority on the basis of GPS-based TSP algorithms. In this study, bus occupancy and schedule adherence were considered as two additional constraints for TSP granting. Specific thresholds were set for the two constraints, with 20 passengers for occupancy and 60 seconds for schedule adherence, such that only buses having 20 or more passengers onboard and running 60 or more seconds behind schedule (schedule checkpoints were set up at the beginning of GPS activation zones) could get signal priority within activation zones. Constraints were set stricter in this study than in usual operations to get more significant results. In the simulation models, the implementation of constraints was enabled by using the interface for the component object model to check bus occupancy and schedule adherence. In actual transit operations, the same functions can be realized through cooperation among GPS, automatic passenger counter, and intelligent dispatching systems.

4.1.4 Simulation Scenarios

To analyze benefits and impacts of the TSP implementation alternatives and BRT along the study corridor, the eight scenarios shown in Table 4.1 were created as VISSIM models. Comparative analysis, described in Section 5, was conducted by using simulation results obtained from the eight scenario models.

Table 4.1 Simulation Scenarios

Number	Scenario	Description
1	Base	Bus Route 33 without TSP, which is the base scenario reflecting existing Route 33 transit operations along the 3300 South corridor, without TSP implementation and without the BRT upgrade
2	TSP	Bus Route 33 with traditional TSP, which introduces traditional TSP with 500-ft detection to Bus Route 33
3	GPS TSP	Bus Route 33 with GPS-based TSP, which introduces GPS-based TSP with a 500-ft activation zone to Bus Route 33
4	BRT	BRT without TSP, which introduces the BRT upgrade with bus stop reduced and relocated, and queue jump lanes added. Buses run at the same 15-min headway in mixed traffic; no TSP is provided in the model.
5	BRT TSP	BRT with traditional TSP, which introduces BRT upgrade with bus stop reduced and relocated, queue jump lanes added, and traditional TSP with 500-ft detection implemented for the BRT line
6	BRT GPS TSP	BRT with GPS-based TSP, which introduces BRT upgrade with bus stop reduced and relocated, queue jump lanes added, and GPS-based TSP with a 500-ft activation zone implemented for the BRT line
7	BRT CTSP	BRT with conditional TSP, which, on the basis of the BRT GPS TSP Model, introduces CTSP that grants signal priority to BRT vehicles within the activation zones according to bus occupancy (with a 20-passenger threshold)
8	BRT CTSP2	BRT with multiconditional TSP, which introduces CTSP with constraints including both bus occupancy and schedule adherence; TSP is only granted to a BRT vehicle within activation zones if the vehicle has more than 20 passengers onboard and is running 60 s or more behind schedule.

4.2 DT Modeling

4.2.1 Genetic Algorithm (GA) for Determining Behavior-Controlled DT

Bus DT is generally influenced by the number of passengers boarding, alighting, or atypical passenger activities (e.g., bike or disabled passenger boarding/alighting). The general consensus of DT modeling distinguishes between sequential and simultaneous boarding and alighting. Sequential model assumes passenger activities (boarding and alighting) occur subsequently, and the DT is modeled as:

$$DT = \sum_{j=1}^A t_j^a + \sum_{j=1}^B t_j^b + \text{deadtime} \quad (2)$$

where A and B represent the number of alighting and boarding passengers, respectively; t_j^a and t_j^b are the times that passenger j takes to alight or board; and dead-time is the time needed to open and close the doors. In case of simultaneous boarding and alighting, where boarding and alighting occur at the same time, DT is modeled as:

$$DT = \max \left\{ \sum_{j=1}^A t_j^a, \sum_{j=1}^B t_j^b, \text{Atypical} \right\} + \text{deadtime} \quad (3)$$

where the notations in Equation (1) still apply.

Based on field observation, the simultaneous model is applicable to 35M BRT. The simultaneous model formulation indicates that the APC/AFC data set for modeling DT needs to be divided into three separate classes: boarding controlled (BC), alighting controlled (AC), and atypical situations. BC refers to

observations where $\max\left\{\sum_{j=1}^A t_j^a, \sum_{j=1}^B t_j^b, Atypical\right\} = \sum_{j=1}^B t_j^b$, AC refers to observations where $\max\left\{\sum_{j=1}^A t_j^a, \sum_{j=1}^B t_j^b, Atypical\right\} = \sum_{j=1}^A t_j^a$, and atypical scenarios refer to observations where $\max\left\{\sum_{j=1}^A t_j^a, \sum_{j=1}^B t_j^b, Atypical\right\} = Atypical$. Separate DT models are needed for each class,

and for this study focused on fare payment effects, the BC observations are of primary interest. Atypical scenarios are defined as scenarios with DT per boarding passenger longer than 10 seconds and DT per alighting passenger longer than five seconds. These values were chosen because they are about twice the estimated time of average passenger activities (see Table 5.4). In addition, our field observation attested that the fastest biker boarding time was approximately 10 seconds. To separate BC and AC datasets, GA was applied to the APC/AFC records in MATLAB. GA is a heuristic search process commonly used to generate solutions for optimization problems. Given an objective function, GA uses a random number generator to populate alternatives at each iteration. The process continues until an optimal solution is reached. The objective function for distinguishing BC and AC data sets was expressed as:

$$GA: \text{minimize } (abs(DT_{estimated_i} - DT_{actual_i})) \quad (4)$$

where;

$$DT_{estimated_i} = \max\left\{\sum_{j=1}^A t_j^a, \sum_{j=1}^B t_j^b\right\} + \text{deadtime} \quad (5)$$

$$\sum_{j=1}^A t_j^a = B_{EFC_i} * T_{EFC_i} + B_{Non-EFC_i} * T_{Non-EFC_i} \quad (6)$$

$$\sum_{j=1}^B t_j^b = A_i * T_{alighting_i} \quad (7)$$

with the following constraints based on previous studies and field observations:

- 2 seconds $\leq T_{EFC_i} \leq$ 8 seconds
- 2 seconds $\leq T_{Non-EFC_i} \leq$ 10 seconds
- 1 seconds $\leq T_{alighting_i} \leq$ 5 seconds
- 1 seconds \leq deadtime \leq 6 seconds

where B_{EFC_i} and $B_{Non-EFC_i}$ are the numbers of boarding passengers with and without smart card payment, respectively, for the i^{th} observation (where one observation is a stop of a bus for boarding and alighting); A_i is the number of alighting passengers for the i^{th} observation; T_{EFC_i} and $T_{Non-EFC_i}$ are average boarding times for smart card users and non-users, respectively, for the i^{th} observation; $T_{alighting_i}$ is average alighting time for the i^{th} observation.

Heuristic searches that are part of GA were used to determine optimal estimates of T_{EFC_i} , $T_{Non-EFC_i}$, and $T_{alighting_i}$ given the defined constraints, and consequently whether the i^{th} observed DT was boarding or alighting controlled. Following this process, 7,725 APC observations were identified as BC, and 3,279 of them were identified as AC. The summary statistics of BC observations are shown in Table 4.2. Given the objectives of this study, these BC observations became the focus of the remainder of the analysis.

Table 4.2 Summary Statistics of Boarding Controlled (BC) Observations

Variable	Obs.	Mean	Std. Deviation	Min	Max	Sum
DT	7725	17.055	13.270	4.8	169.8	-
Weekend	7725	0.084	0.277	0	1	-
B-EFC	7725	0.263	0.610	0	8	2033
B-CTVM	7725	2.689	2.282	0	18	20692
A-EFC	7725	0.051	0.235	0	3	396
A-CTVM	7725	0.917	1.443	0	16	7087
Door-Cycle	7725	1.288	0.496	0	5	-
Fair-Mall stop (Magna direction)	7725	0.083	0.276	0	1	-
3575 W stop	7725	0.035	0.185	0	1	-
3955 W stop	7725	0.059	0.235	0	1	-
Fair-Mall stop (TRAX direction)	7725	0.035	0.183	0	1	-
1685 W stop	7725	0.049	0.215	0	1	-

- DT: measures the time (in seconds) between when first doors open to last doors close.
- B-EFC: number of passengers boarding using electronic fare payment, or number of passengers who use electronic fare collection (EFC) method, recorded by AFC.
- A-EFC: number of passengers alighting using EFC, recorded by AFC.
- B-CTVM: number of boarding passengers using non-electronic fare payment.
- A-CTVM: number of alighting passengers using non-electronic fare payment.
- Weekend: indicator that shows whether the observation is on weekend (1) or on weekday (0).
- Door-Cycle: shows how many time bus doors were opened and closed during the observation, recorded by APC.
- Stop-[station name]: indicator shows the station at which the observation was collected. These specific stations are presented in the table because of their ultimate significant impact on DT (see Tables 5.4 and 5.6), with other stations showing no unique effects.

4.2.2 DT Modeling and Fare Payment Structure Analysis

After categorizing all APC observations, atypical scenarios were excluded from the modeling effort as they might contain irreproducible features or belong to rare situations. In order to estimate the fare payment structure and their impact on DT, especially those methods that do not have an electronic footprint, BC-related APC observations were used in the analysis from this point forward. AC-related data were excluded because both on-board cash payers and prepaid pass holders share the same alighting behavior (no tap-off or transaction-related activity required) whereby additional information for separating these two fare payment methods can be obtained from BC-related APC records (e.g., different boarding or transaction time).

Multivariate regression was adopted for DT modeling in this study. DT was represented as a linear collective function of independent variables, expressed as:

$$DT_i = \beta * X_i + \varepsilon_i \quad (8)$$

where DT_i is DT for the i^{th} observation, β is a vector of estimable coefficients, associated with each right-hand-side variable X_i is the vector of measurable characteristics that determine DT for the i^{th} observation, and ε_i is the disturbance term. X_i in Equation (8) includes all the variables in Table 4.2 plus a constant term (dead-time). Therefore, the model can be rewritten as:

$$\begin{aligned}
DT_i = & \beta_{Weekend} * Weekend_i + \beta_{BEFC} * BEFC_i + \beta_{BCTVM} * BCTVM_i + \beta_{AEFC} \\
& * AEFC_i + \beta_{ACTVM} * ACTVM_i + \beta_{DoorCycle} * DoorCycle_i \\
& + \beta_{Fair-Mall\ stop\ (Magna\ direction)} \\
& * FairMall\ stop\ (Magna\ direction)_i + \beta_{3575\ W\ stop} \\
& * 3575\ W\ stop_i + \beta_{3955\ W\ stop} * 3955\ W\ stop_i \\
& + \beta_{Fair-Mall\ stop\ (TRAX\ direction)} \\
& * FairMall\ stop\ (TRAX\ direction)_i + \beta_{1685\ W\ stop} \\
& * 1685\ W\ stop_i + C + \varepsilon_i
\end{aligned} \tag{9}$$

where $\beta_{variable\ name}$ is the parameter estimates associated with that particular right-hand-side variable, $Station\ Name_i$ is the station dummy variable indicating the station of the i^{th} observation, and C is the constant term representing the portion of dead-time that the driver spent to ensure the door area was cleared.

In Equation (9), B-CTVM accounts for the total number of prepaid pass holders (B-TVM) and on-board cash payers (B-Cash). To distinguish the two sets of the passenger population based on fragmented APC data, search algorithm were applied. Assume all the independent variables in the model are fixed in repeated samples and therefore independent of the error term, their parameter estimates should remain the same when B-CTVM is replaced with B-TVM and B-Cash. As a result, Equation (9) can be further rewritten as:

$$\begin{aligned}
DT_i = & \beta_{Weekend} * Weekend_i + \beta_{BEFC} * BEFC_i + \beta_{BCTVM} * BCTVM_i + \beta_{BCash} \\
& * BCash_i + \beta_{AEFC} * AEFC_i + \beta_{ACTVM} * ACTVM_i + \beta_{DoorCycle} \\
& * DoorCycle_i + \beta_{Fair-Mall\ stop\ (Magna\ direction)} \\
& * FairMall\ stop\ (Magna\ direction)_i + \beta_{3575\ W\ stop} \\
& * 3575\ W\ stop_i + \beta_{3955\ W\ stop} * 3955\ W\ stop_i \\
& + \beta_{Fair-Mall\ stop\ (TRAX\ direction)} \\
& * FairMall\ stop\ (TRAX\ direction)_i + \beta_{1685\ W\ stop} \\
& * 1685\ W\ stop_i + C + u_i
\end{aligned} \tag{10}$$

From Equations (9) and (10), the following can be concluded:

$$\beta_{BCTVM} * BCTVM_i + \varepsilon_i = \beta_{BCash} * BCash_i + \beta_{BCTVM} * BCTVM_i + u_i \tag{11}$$

where β_{BCash} and β_{BCTVM} are the parameter estimates associated with B-Cash and B-TVM variables, respectively, and u_i is the error term of the i^{th} observation in the updated model.

The optimal OLS model will yield an estimate for β_{BCTVM} . Yet given the unavailability of data, $\beta_{BCash}, BCash_i, \beta_{BCTVM}, BCTVM_i, BCash_i$ are unknown in Equation (11). Thus, GA was used again to estimate the fare payment structure and their individual impacts on DT.

The optimization problem for determining the fare payment structure can be expressed as:

$$\begin{aligned}
GA: \min[abs\{(\beta_{B_{CTVM}} * B_{CTVM_i} + \varepsilon_i) - (\alpha_{B_{Cash_i}} * B_{Cash_i} + \alpha_{B_{TVM_i}} * B_{TVM_i})\}] & \quad (12a) \\
\text{subject to } B_{Cash_i}, B_{TVM_i} \in \mathbb{Z} & \quad (12b) \\
B_{CTVM_i} = B_{Cash_i} + B_{TVM_i} & \quad (12c) \\
\beta_{B_{Cash}} > \beta_{B_{CTVM}} > \beta_{B_{TVM}} & \quad (12d) \\
\text{Slowest } B_{TVM} > \alpha_{B_{TVM_i}} > \text{Fastest } B_{TVM} & \quad (12e) \\
\text{Slowest } B_{Cash} > \alpha_{B_{Cash_i}} > \text{Fastest } B_{Cash} & \quad (12f) \\
\text{Average } \alpha_{B_{TVM_i}} \cong \beta_{B_{TVM}} & \quad (12g) \\
\text{Average } \alpha_{B_{Cash_i}} \cong \beta_{B_{Cash}} & \quad (12h) \\
u_i = 0 & \quad (12i)
\end{aligned}$$

where $\alpha_{B_{TVM_i}}$ and $\alpha_{B_{Cash_i}}$ are the average boarding time for B-TVM and B-Cash, respectively, Slowest B-TVM/B-Cash (Fastest B-TVM/ B-Cash) refers to the maximum (minimum) average boarding time for prepaid pass holders and onboard cash payers, separately; and other notations remain the same as previously defined.

Constraints (12b) and (12c) are integrality constraints and assure that the number of onboard cash payers and prepaid pass holders totals to B-CTVM. Constraints (12d) through (12f) are set on the basis of previous studies and our field observations. They ensure that the average boarding time for prepaid pass holders is shorter than onboard cash payers given the assumption that no additional interaction exists with their boarding. The approximate equivalence between $\beta_{B_{TVM}} / \beta_{B_{Cash}}$ and $\alpha_{B_{TVM_i}} / \alpha_{B_{Cash_i}}$ given by constraints (12g) and (12h) assures that the variability of the boarding time for each observation is fully captured. Constraint (12i) is proven in the following proposition: if the optimal OLS model includes all the independent variables that affect DT, except for B-Cash and B-TVM, then ε_i in Equation (11) solely captures the variability introduced by B-Cash and B-TVM. Thus, by including these two variables into the updated model (Equation 11), the new error term $u_i \sim 0$, as there exists no other unexplained variation for DT.

By applying GA to solve Equation (12a), the result provides estimates for B-Cash and B-TVM for each individual observation. Thus, the parameters in Equation (10) can be estimated using OLS to quantitatively identify the impacts of all the variables on DT.

5. RESULTS AND DISCUSSION

5.1 TSP Microscopic Simulation

Outputs from the eight simulation scenarios included signalized intersection performance, travel times, and network performance measures. To estimate the benefits and impacts of different combinations of TSP strategies and BRT upgrades, the output data were analyzed from the perspectives of transit operations, non-transit operations along the corridor, and non-transit operations along side streets. All comparisons performed had their significance examined by using statistical tests (*t*-test and analysis of variance).

5.1.1 Transit Travel Time

Compared with that of the base model, the transit travel time was shorter in the TSP model and GPS-based TSP model. The average eastbound transit travel time decreased by 8.7% with traditional TSP and 9.6% with GPS-based TSP, while the average westbound transit travel time decreased by 8.4% with traditional TSP and 8.2% with GPS-based TSP. As the detection distance was set to 500 feet in both models, no significant differences were found in the effectiveness of traditional TSP and GPS-based TSP. This finding was supported by the similar travel time reductions in the two models compared with the base. The BRT upgrade was effective in reducing transit travel time because of the reduced number of bus stops. Additional benefits came from the queue jump lanes, an additional preferential treatment provided for the BRT buses. With the BRT upgrade, the average transit travel time decreased by 29.3% in eastbound trips and 34.1% in westbound trips compared with the base scenario.

With TSP, the BRT travel time decreased further. Compared with the BRT model, the average eastbound transit travel time fell by 11.2% in the BRT TSP model, by 8.8% in the BRT GPS TSP model, by 6.7% in the BRT CTSP model, and by 3.0% in the BRT CTSP2 model. The average westbound transit travel time also fell by 9.1%, 4.2%, 6.4%, and 0.8%, respectively, in these same four scenarios. With TSP constraints, the reductions in travel time were not as significant as with unconditional TSP scenarios. Figure 5.1 shows the eastbound and westbound transit travel time results from the eight simulation models, segment by segment.

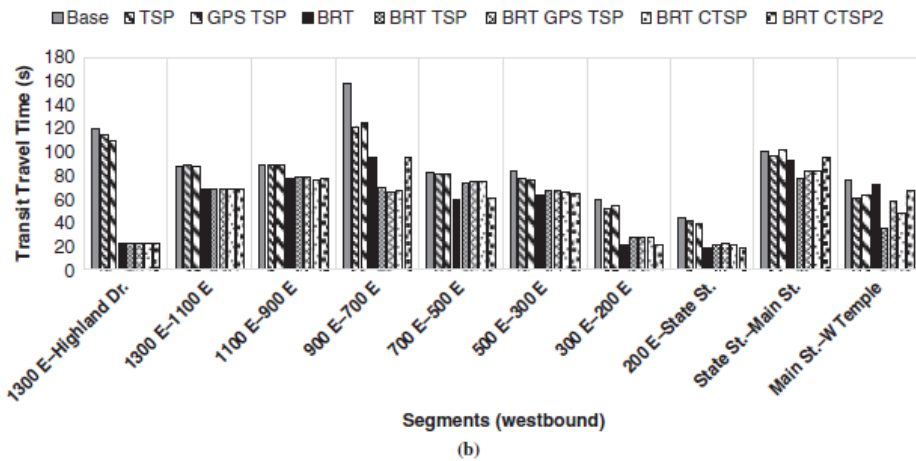
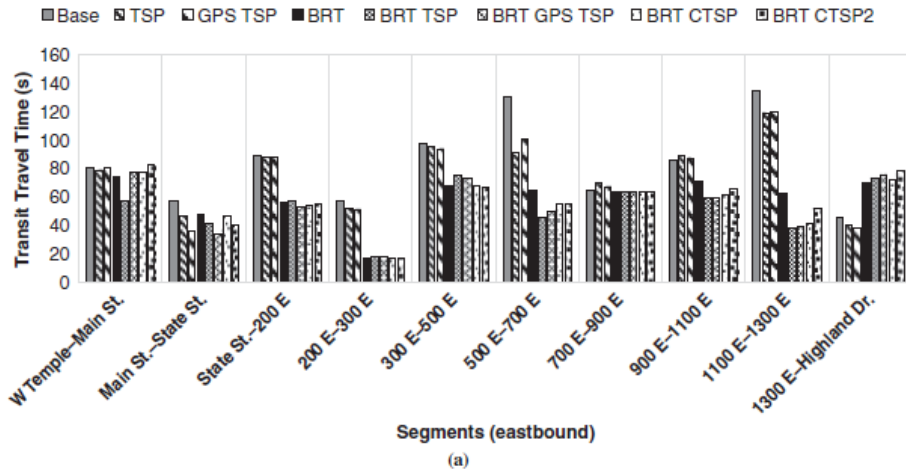


Figure 5.1 Transit Travel Times: (a) Eastbound and (b) Westbound (W = west; E = east)

For some critical segments on which regular buses had been running slowly, average transit travel times decreased quite significantly after TSP and BRT implementations. Table 5.1 shows the two-hour total transit delays expressed in vehicle delay and person delay. The Δ /base row in the table shows that significant reductions occurred in total transit delay in Scenarios 2 to 8 compared with the base model. In addition, the Δ /BRT row shows significant reductions in total transit delay from Scenarios 6 and 7 compared with the BRT model. These results are consistent with the transit travel time results, and they show that BRT upgrades have significant effects on reducing transit delays. The CTSP strategies are not as effective as unconditional TSP strategies are in reducing transit delays because CTSP strategies grant priority only to transit vehicles that satisfy the given constraints.

Table 5.1 Total Transit Delays for 2-hour Simulation

Delay	Base	TSP	GPS TSP	BRT	BRT TSP	BRT GPS TSP	BRT CTSP	BRT CTSP2
Vehicle								
2-h total (h)	1.9	1.6	1.6	1.2	0.9	1.0	1.0	1.2
Δ /Base ^a (%)	na	-17	-18	-38	-53	-46	-46	-40
Δ /BRT ^b (%)	na	na	na	na	-24	-13	-13	-3
Person								
2-h total (h)	46.7	38.2	38.1	30.2	22.6	25.6	-24.6	28.6
Δ /Base ^a (%)	na	-18	-18	-35	-52	-45	-47	-39
Δ /BRT ^b (%)	na	na	na	na	-25	-16	-19	-5

NOTE: na = not applicable.

^a Δ /Base = percentage of change in transit delay compared with base model.

^b Δ /BRT = percentage of change in transit delay compared with BRT model.

5.1.2 Non-transit Travel Time

Compared with those of the base model, the non-transit travel times did not change significantly with TSP strategies and BRT upgrades. In eastbound and westbound trips, the average non-transit travel times changed by amounts ranging from -2.3% to +1.0%. This change resulted from the relatively much larger non-transit volume than transit volume. The additional green seconds or reduced red seconds brought by TSP did not affect the majority of the non-transit traffic along the corridor. Figure 5.2 shows the eastbound and westbound non-transit travel time resulting from the eight simulation models, segment by segment. Apart from some slight changes on a few critical segments where traffic had been moving slowly, the average non-transit travel times remained relatively steady in the eight scenarios.

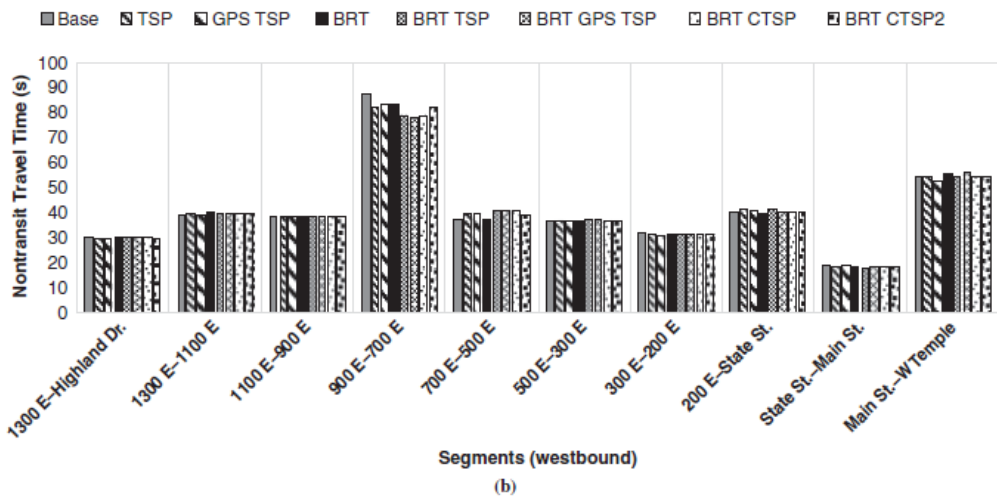
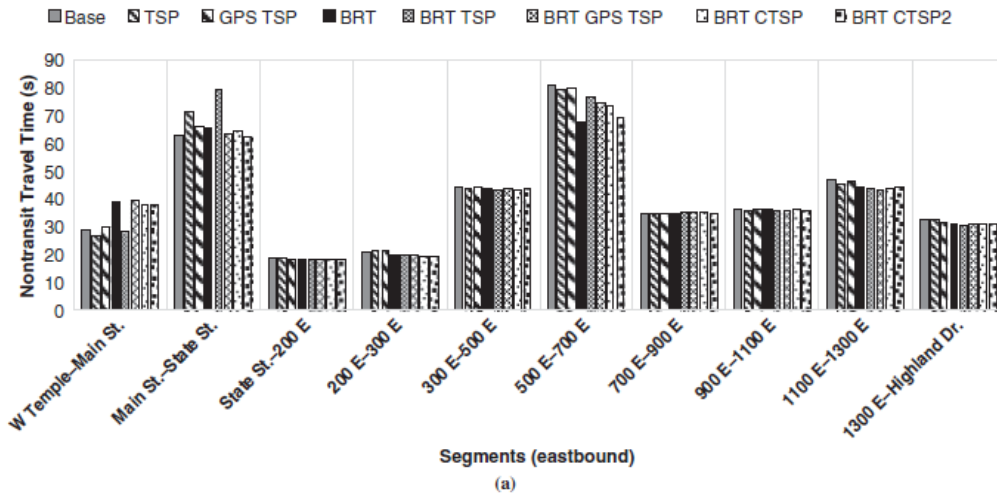


Figure 5.2 Non-transit Travel Time: (a) Eastbound and (b) Westbound

5.1.3 Impacts on Side-Street Traffic

When TSP is provided along a main corridor, green extension and early green facilitate transit operations along that corridor and may increase side-street traffic delays. Table 5.2 shows the two-hour total side-street traffic delays in vehicle delay and person delay. Compared with those delays of the base model, the TSP and GPS-based TSP strategies resulted in significant delay increases (up to 6%) in vehicle and person delays experienced by side-street traffic. BRT upgrades had no additional impacts on side-street traffic delays because those upgrades (bus stop reductions and relocations and queue jump lanes) did not have direct impacts on traffic signal timing. Compared with the BRT model, the add-in of TSP strategies in the BRT scenario increased side-street traffic delays. However, the multi-conditional TSP (CTSP2) strategy helped to keep the impacts on side-street traffic delay at approximately the same level as those of the base model and the BRT model.

Table 5.2 Total Side-Street Traffic Delays for 2-hour Simulation

Delay	Base	TSP	GPS TSP	BRT	BRT TSP	BRT GPS TSP	BRT CTSP	BRT CTSP2
Vehicle								
2-h total (h)	270.3	285.1	285.9	269.8	276.2	276.6	274.9	271.9
Δ /Base ^a (%)	na	6	6	0	2	2	2	1
Δ /BRT ^b (%)	na	na	na	na	2	3	2	1
Person								
2-h total (h)	323.9	340.5	341.8	321.6	329.4	329.3	327.7	323.4
Δ /Base ^a (%)	na	5	6	-1	2	2	1	0
Δ /BRT ^b (%)	na	na	na	na	2	2	2	1

^a Δ /Base = percentage of change in side-street traffic delay compared with base model.

^b Δ /BRT = percentage of change in side-street traffic delay compared with BRT model.

Figure 5.3 shows both the average queue lengths and the average number of stops per vehicle on side streets. Figure 5.3a shows that the average queue lengths increased on some critical side streets, such as 700 East and 1300 East, with TSP and BRT implementations compared with the base model. These two side streets, under existing conditions, already had longer traffic queues than the others. Therefore, the introduction of TSP strategies and BRT upgrades along the 3300 South corridor may worsen this situation. Figure 5.3b indicates that the average number of stops per vehicle did not change significantly across the eight scenarios.

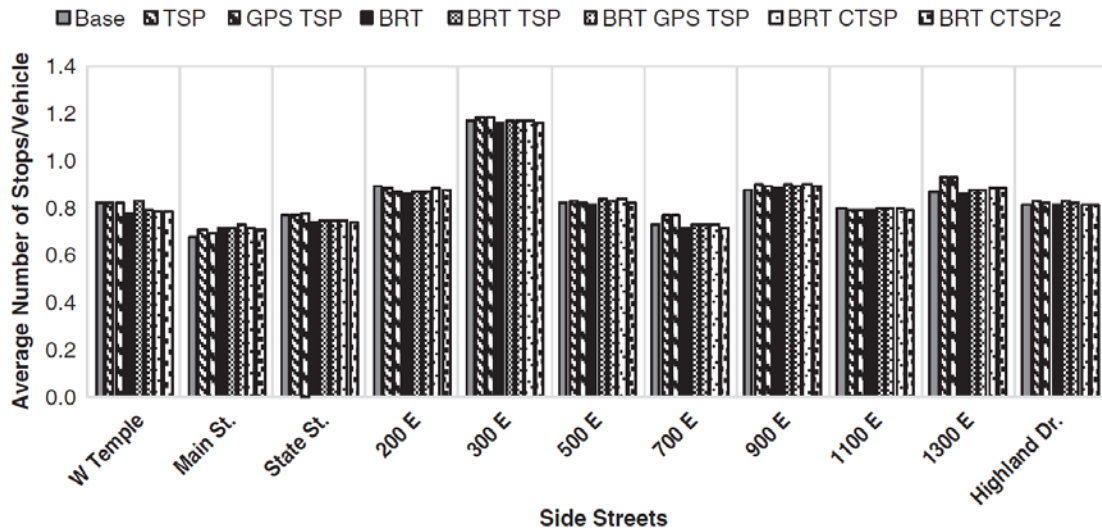
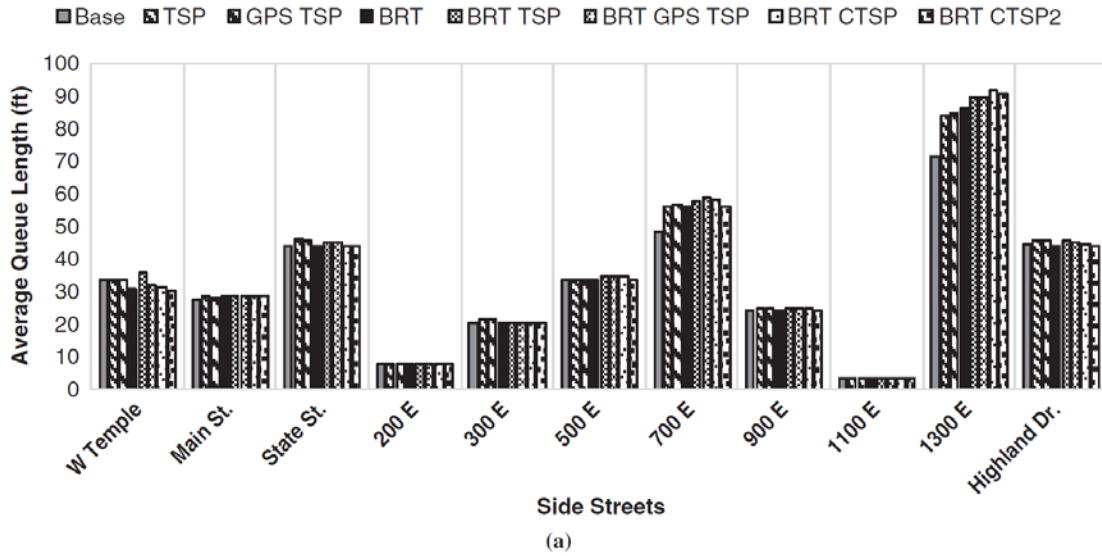


Figure 5.3 Data for Side-Streets: (a) Average Queue Lengths and (b) Average Number of Stops per Vehicle

5.1.4 Network Performance

Table 5.3 shows the transit and non-transit network performance results from the eight simulation models. The vehicle number indices and traveled distances show that the inputs to the eight models were consistent. The delay results were consistent with the previous analysis reported in this paper. The stop delay indices show the impacts of TSP strategies and BRT upgrades on traffic movements at an entire-network level. Average transit speed increased significantly with BRT upgrades. TSP strategies also helped to improve this value to a lesser extent. Average non-transit speed remained relatively steady at 19 to 21 mph. The total transit travel time, as analyzed in the earlier section on transit travel time, revealed the effectiveness of different combinations of TSP strategy and BRT on transit operations.

Table 5.3 Transit and Non-transit Network Performances

Characteristic	Base	TSP	GPS TSP	BRT	BRT TSP	BRT GPS TSP	BRT CTSP	BRT CTSP2
Transit								
Number of vehicles in network	3	3	3	2	2	2	2	2
Number of vehicles that have left network	15	15	15	16	16	16	16	16
Total vehicles	18	18	18	18	18	18	18	18
Average delay time per vehicle (s)	506.17	438.33	442.03	342.57	284.04	306.48	309.59	334.06
Total delay time (h)	2.53	2.19	2.21	1.71	1.42	1.53	1.55	1.67
Average stopped delay per vehicle (s)	185.16	127.85	130.40	120.93	66.22	83.72	86.79	117.78
Total stopped delay (h)	0.93	0.64	0.65	0.60	0.33	0.42	0.43	0.59
Average number of stops per vehicle	10.32	9.30	8.91	8.42	7.76	8.13	8.20	7.92
Number of stops	185.80	167.40	160.40	151.60	139.60	146.40	147.60	142.60
Average speed (mph)	10.23	10.96	10.93	14.02	15.15	14.71	14.65	14.19
Total travel time (h)	5.32	4.99	5.01	3.93	3.63	3.75	3.76	3.89
Total distance traveled (mi)	54.38	54.69	54.72	55.09	55.04	55.14	55.13	55.22
Nontransit								
Number of vehicles in network	979	984	1,010	1,021	958	1,053	1,030	1,007
Number of vehicles that have left network	30,241	30,235	30,866	30,872	30,261	30,834	30,870	30,883
Total vehicles	31,220	31,219	31,876	31,894	31,219	31,887	31,900	31,889
Average delay time per vehicle (s)	62.52	63.66	64.24	74.12	62.67	80.16	75.51	74.40
Total delay time (h)	673.32	685.64	706.48	815.04	675.06	881.46	830.42	818.10
Average stopped delay per vehicle (s)	41.91	42.67	43.05	46.22	41.86	48.47	46.93	46.23
Total stopped delay (h)	451.40	459.52	473.44	508.23	450.89	532.94	516.17	508.39
Average number of stops per vehicle	1.55	1.56	1.57	1.84	1.55	1.95	1.86	1.84
Number of stops	59,942.40	60,653.20	62,291.00	72,771.20	60,112.80	77,332.00	73,688.40	72,853.80
Average speed (mph)	21.05	20.92	20.84	19.75	21.03	19.13	19.61	19.71
Total travel time (h)	1,869.39	1,881.78	1,929.46	2,036.68	1,871.72	2,102.19	2,051.94	2,040.16
Total distance traveled (mi)	39,354.79	39,357.98	40,205.33	40,176.87	39,365.64	40,150.65	40,175.31	40,193.98

5.2 Results of DT Modeling and Fare Payment Structure Analysis

Following the modeling process presented in Section 4.2, the result of the optimal OLS model with B-CTVM is shown in Table 5.4. The parameters associated with all of the independent variables are statistically significant, and the model shows acceptable goodness-of-fit with an adjusted R-squared of 0.59. As shown in Table 5.4, DT is a function of Weekend, B-EFC, B-CTVM, A-EFC, A-CTVM, Door-Cycle, five different individual stop indicators, and an intercept. Even though the model used only BC-related APC observations, it is noted that the impact of alighting passengers was statistically significant. This is largely because, in reality, there rarely exists perfect simultaneous or sequential boarding and alighting. The optimal model was selected through extensive specification testing to find the most logical and informative model.

Table 5.4 Optimal Model Specification with B-CTVM

R-squared =	0.5943			
Adjusted R-squared =	0.5937			
F(11, 7713) =	1027.05			
Prob > F =	0.00			
DT	Coefficient	Std. Error	t	P> t
Weekend *	1.411	0.349	4.04	0.000
B-EFC *	4.992	0.163	30.64	0.000
B-CTVM *	3.329	0.047	71.46	0.000
A-EFC *	2.623	0.418	6.28	0.000
A-CTVM *	1.741	0.075	23.14	0.000
Door-Cycle *	1.580	0.196	8.06	0.000
Fair-Mall stop indicator (Magna dir.) *	2.478	0.390	6.36	0.000
3575 W stop indicator *	-2.598	0.525	-4.95	0.000
3955 W stop indicator *	2.222	0.413	5.38	0.000
Fair-Mall stop indicator (TRAX dir.) *	3.766	0.560	6.72	0.000
1685 W stop indicator *	2.479	0.456	5.44	0.000
Constant *	2.411	0.290	8.32	0.000

*: 99% confidence level

To further replace B-CTVM with the estimated number of prepaid pass holders and onboard cash payers, Equation (12a) was solved with GA. The constraints (12e) and (12f) needed to be further defined based on field observation and the literature. TCQSM provides an estimated boarding time range of 1.75-2.5 seconds/passenger with no fare payment (which is similar to prepaid pass holders, transfer ticket holders, or fare evaders), and 3.1-8.4 seconds/passenger with on-board cash payment (TRCP, 2013). Additionally, our field observations indicated that boarding time for prepaid pass holders took up to 4.5 seconds/passenger. The optimal model result presented in Table 5.4 for B-CTVM (3.3 seconds/passenger) was used to further define the lower boundary for onboard cash payers. Thus, constraints (12e) and (12f) were updated as:

$$4.3 \text{ seconds} > \alpha_{B_TVM_i} > 1.3 \text{ seconds} \quad (13)$$

$$7.3 \text{ seconds} > \alpha_{B_Cash_i} > 3.3 \text{ seconds} \quad (14)$$

GA thereby yielded the estimated number of cash payers and prepaid pass holders for each APC observation (B-Cash and B-TVM). Summary statistics of the results are shown in Table 5.5.

Table 5.5 Summary Statistics of B-Cash and B-TVM

Variable	Obs.	Mean	Std. Deviation	Min	Max	Sum
B-TVM	7725	1.743	2.163	0	18	13467
B-Cash	7725	0.935	1.605	0	12	7225

The outcome presented in Table 5.5 was integrated in the OLS model for a new coefficients estimation of DT, where B-CTVM was replaced with B-Cash and B-TVM, as explained in Equation (9). The final model specification is shown in Table 5.6.

Table 5.6 Final Optimal Model Specifications with B-TVM and B-Cash

R-squared =				0.9011
Adjusted R-squared =				0.9009
F(12, 7712) =				5852.99
Prob > F =				0.00
DT	Coefficient	Std. Error	t	P> t
Weekend *	1.087	0.173	6.30	0.000
B-EFC *	5.279	0.081	65.57	0.000
B-TVM *	1.803	0.025	73.03	0.000
B-Cash *	6.917	0.033	211.68	0.000
A-EFC *	2.020	0.206	9.79	0.000
A-CTVM *	1.611	0.037	43.40	0.000
Door-Cycle *	1.509	0.097	15.60	0.000
Fair-Mall stop indicator (Magna dir.) *	2.116	0.192	11.00	0.000
3575 W stop indicator *	-2.588	0.259	-9.98	0.000
3955 W stop indicator *	1.617	0.204	7.92	0.000
Fair-Mall stop indicator (TRAX dir.) *	3.432	0.277	12.40	0.000
1685 W stop indicator *	2.287	0.225	10.15	0.000
Constant*	2.026	0.143	14.15	0.000

*: 99% confidence level

The final model demonstrates excellent goodness-of-fit with an adjusted R-squared of 0.90. Parameters associated with all the variables in the specification are statistically significant. In the sections to follow, result interpretation were discussed in length and potential estimation concerns arising from the GA assumptions presented are addressed by conducting validity testing.

5.2.1 Result Interpretation

The final DT model showed good statistical fit with an adjusted R-squared of 0.90. All estimated variable coefficients were statistically significant and had plausible signs. The model interpretation and implications are discussed below.

Boarding

The average estimated boarding time for EFC users was around 5.2 seconds/passenger, which was much longer than the suggested time (2.75 seconds) by TCQSM (TCRP, 2013). Two possible reasons may contribute to the difference: the tap on/tap off EFC reader on the UTA fleet has slower refresh rates compared with the common smart card reader systems used in the U.S.; and a significant portion of EFC users delayed their boarding process by searching for the card (according to field observations).

The average boarding time for passengers who use prepaid passes, transfer tickets, or fare evasion was about 1.8 seconds/passenger, which matches the TCQSM suggestion (1.75 seconds/passenger) (TCRP, 2013). Average boarding time for passengers who paid their fare by cash was about 6.9 seconds/passenger, which was approximately 2.5 seconds/passenger longer than what TCQSM suggested (4.5 seconds/passenger). This difference may largely be due to the fact that a sizable portion of passengers did not have the exact cash ready before boarding. The boarding time for on-board fare payers (including

cash payers and smart card users) were considerably higher than off-board fare payers (prepaid pass holders and transfer ticket users). By eliminating the onboard cash payment on 35M BRT (assuming that all cash payers will switch to prepaid passes), DT can be reduced by at least 30 minutes/day just for BC related observations.

Alighting

Due to the nature of data used for DT modeling, only BC-related APC observations were used in this study. Thus, it was expected that the alighting time in our model be lower than TCQSM's suggestion, given the limited impact of alighting time in the data used for model estimation. The average alighting time for EFC users and non-EFC users was 2.0 seconds/passenger, and 1.6 seconds/passenger, respectively, which are indeed less than TCQSM suggested alighting time (3.5 and 1.75 seconds/passenger, respectively).

Stop Characteristics

One of the critical factors affecting DT that is often neglected in most previous published studies is stop placement, design, and built environment. The large sample of data provided by APC offered a unique opportunity to explore the impact of stop characteristics on DT to an extent allowable by the data characteristics.

The parameter estimates for fair-mall stop indicator showed that, on average, the DT is 2.1 seconds (for Magna direction) and 3.4 seconds (for TRAX direction) longer than other stops. This is highly likely due to the longer service time required for passengers carrying shopping bags. A shorter expected DT (by 2.6 seconds) was estimated for the 3527 W stop. Being the only stop along the route placed on the roadway median, the built environment appears to better prepare passengers for an effective boarding. The 3955 W stop suffered from longer expected DT (2.2 seconds more) possibly since it is close to a hospital. Possibly due to its nature serving as a transfer stop, 1685 W had a longer expected DT (2.5 seconds) as bus drivers tend to intentionally elongate the boarding time for passengers to complete their transfer between Bus Route 217 and 35M.

Dead-Time

Dead-time consists of the time for door opening and closing and any additional time consumed. The DT model incorporated dead-time by including the door cycle variable and the constant term (*C*). Based on the model estimation results shown in Table 5.6, dead-time can be expressed as:

$$Dead\ Time = 1.5 * DoorCycle + 2 \quad (16)$$

In reality, the door is open/closed at least once at each stop (that has a DT). Thus, the minimum estimated dead-time was 3.5 seconds.

Miscellaneous Factors

Miscellaneous variables that could affect DT, such as time-of-day, day-of-week, and crowding effects, were also explored. Day-of-week yielded statistically insignificant effects on DT according to the model; however, it does predict that weekends are prone to have longer expected DTs.

In order to capture the crowding effect, different variables such as *Crowding Variable* = $(passenger\ load - seating\ capacity)^2 * (Barding + Alighting)$ used by Milkovits (18) were tested in the model. However, the crowding variables were determined to either not be statistically significant or

not have logically meaningful impact on DT. Data analysis showed that only 148 out of 7,725 (1.9%) BC observations experienced a load of more than 28 passengers (seating capacity). Approximately only 0.1% of BC observations experienced a load exceeding 58% of capacity (35 passengers), which was used as a threshold for identifying crowding effect in many studies (60% of capacity). Thus, crowding rarely occurred on 35M. Analysis also showed that in the model, time-of-day only had limited impact on DT, which is consistent with the finding presented in Rajbhandari et al. (2003).

5.2.2 Testing Model Validity

Three posterior tests are conducted for model diagnosis and to ensure its validity.

Seemingly Unrelated Estimation Test

Seemingly unrelated estimation test (Weesie, 1999) was applied to both models presented in Tables 5.5 and 5.6. The purpose of the test, similar to Hausman specification test (Hausman, 1978), was to assess the consistency of parameter estimates of the common variables. A seemingly unrelated estimation system comprises of several individual relationships that are linked by the fact that their disturbances are correlated. Its typical applications are tests for intra-model and cross-model hypotheses. In our modeling context, the null hypothesis is that all the parameter estimates of the common variables in the two models are equal. The results ($\chi^2 = 8.09$, $\text{Pr} > \chi^2 = 0.62$) indicates the consistence of the coefficients of common variables in the two models (do not reject the null hypothesis). This suggests that the estimated coefficients of B-Cash and B-TVM do not capture additional impact on DT from other variables, thus solely represent B-CTVM.

Model Testing and Validation

The developed DT model (shown in Table 5.6) was applied to the testing data set for performance assessment. Using the APC/AFC data collected on February 10, 2015, GA presented in Equation (11) was solved for estimation of B-Cash and B-TVM. The result was compared against 120 manually collected records. The GA estimation matched ground truth data in 110 observations (92%), and the rest had minimal errors (one passenger bias). The error was usually caused by the fact that not all the cash boarding followed the upper and lower boundaries set in the model. For example, sometimes cash payment transaction for the last passenger was completed after the bus started moving, which goes beyond the assumed lower boundary for cash payers. The total number of estimated B-Cash was approximately 10% higher than the ground truth data in these cases.

Testing for Possible Bias in Parameter Estimation

Coefficient estimation error introduces bias in the model, and when used for prediction, can result in imprecise forecasting. The purpose of this test was to determine the magnitude of this possible bias in the estimated parameters. The model validation process showed that error occurs when the estimating the number of cash payers and prepaid pass holders when comparing against ground truth data (within 10% difference of number of cash payers), introducing measurement error in these right-hand-side variables. Measurement error in right-hand-side variables can result in bias of the OLS estimator. To explore this further, an error range of [-15%, 15%] of total B-Cash was chosen to assess the impact of measurement error in the right-hand-side variables on coefficient estimates ($\beta_{B_{Cash}}$ and $\beta_{B_{TVM}}$) using sensitivity analysis. A B-Cash value for each observation was randomly populated within the possible range. This was achieved by setting the threshold:

$$B_{cash} = \begin{cases} B_{cash} + \frac{\alpha}{|\alpha|} & \text{if } 0 < \mu < |\alpha| \\ B_{cash} & \text{otherwise} \end{cases} \quad (15)$$

where μ is a random number chosen between [0,1] for each observation, and α is the error range. The number of B-TVM were then updated based on new, randomly drawn B-Cash.

The OLS model presented in Table 5.6 was then estimated to determine DT on the basis of the updated B-Cash and B-TVM. After 100 iterations, the upper and lower boundaries of the estimated coefficients $\beta_{B_{cash}}$ and $\beta_{B_{TVM}}$ are shown in Table 5.7.

Table 5.7 Estimation Error Impact on B-TVM and B-Cash Coefficients

Model	Number of tests	Parameter estimates	Lowest value (seconds/passenger)	Highest value (seconds/passenger)
15% less cash boarding	100	$\beta_{B_{TVM}}$	1.806	1.901
		$\beta_{B_{Cash}}$	6.901	7.086
15% more cash boarding	100	$\beta_{B_{TVM}}$	1.712	1.796
		$\beta_{B_{Cash}}$	6.746	6.965

Note that the impact of B-Cash and B-TVM measurement error is evident in the ranges of estimates for $\beta_{B_{Cash}}$ and $\beta_{B_{TVM}}$, and could therefore negatively impact the accuracy of DT predictions. As an example, $\beta_{B_{Cash}}$ is in the range of [6.7, 7.1]. For the worst-case scenario where the number of onboard cash payers reaches its maximum (B-Cash=12), the resulting bias in DT estimation from a 15% measurement error in the right-hand-side variables is less than 4.8 seconds, which is only about 5% of the actual DT (91s). The magnitude of bias in parameter estimates resulting from this GA estimation is thus considered acceptable.

6. CONCLUSIONS

6.1 TSP Performance Assessment vs. Microscopic Simulation

The objective of this study was to evaluate the corridor-level effectiveness and impacts of GPS-based TSP strategies with mixed-traffic BRT upgrades. The study was based on the proposed 3300 South BRT route in Salt Lake County. Microscopic simulation was used as the main analysis tool. Eight simulation scenarios were created to evaluate different TSP strategies and BRT upgrade combinations. The eight models were (a) the base model reflecting existing conditions, (b) the TSP model with regular bus operations and traditional TSP strategy, (c) the GPS TSP model with regular bus operations and GPS-based TSP strategy, (d) the BRT model with BRT upgrades and no TSP, (e) the BRT TSP model with BRT upgrades and traditional TSP strategy, (f) the BRT GPS TSP model with BRT upgrades and GPS-based TSP strategy, (g) the BRT CTSP model with BRT upgrades and conditional TSP strategy, and (h) the BRT CTSP2 model with BRT upgrades and multi-conditional TSP strategy.

From the analysis results, the benefits of GPS-based TSP were as follows:

- GPS-based TSP strategies can provide transit delay reductions and travel time savings as effective as those of traditional TSP tools with fixed or distance-limited detection. However, the GPS-based TSP strategy is more advanced because of its flexibility in setting and adjusting detection–activation distances, its extensible features, and its relatively lower equipment costs (when most of the transit vehicles have been equipped with GPS).
- In a mixed-traffic BRT system (optimization of bus stop locations and provision for queue jump lanes) with unconditional GPS-based TSP strategy, CTSP strategy considering bus occupancy, and CTSP2 strategy considering bus occupancy and schedule adherence, the total reduction in peak hour transit delay can be, respectively, 13%, 13%, and 3% compared with BRT alone; and the total savings in peak hour transit travel time in those same three scenarios can be, respectively, up to 9%, 7%, and 3% compared with BRT alone.

The impacts of GPS-based TSP strategy were as follows:

- The average non-transit travel time along the study corridor had no significant differences between a base scenario (existing conditions), a scenario with TSP strategies added, and a scenario with BRT upgrades made.
- In a regular bus system, with traditional TSP and GPS-based TSP strategies, the total delays for peak hour side-street traffic increased by 6% compared with existing conditions.
- In a mixed-traffic BRT system (optimization of bus stop locations and provision for queue jump lanes), with strategies of unconditional GPS-based TSP, CTSP considering bus occupancy, and CTSP2 considering bus occupancy and schedule adherence, the total delays for peak hour side-street traffic increased, respectively, by 3%, 2%, and 1%, compared with BRT alone.
- TSP strategy and BRT can increase the average queue lengths on critical side streets, but in general, the impact on queue lengths was minor. No significant impacts on the average number of stops on side streets were seen.

To summarize, unconditional GPS-based TSP strategy performed as effectively as did traditional TSP. However, TSP strategy provided transit delay reductions and travel time savings to a lesser extent than the much more effective BRT upgrades. The TSP strategy alone, however, was still an effective strategy for improving transit operations, as multiple studies have demonstrated. Additionally, when the higher flexibility, higher extensibility, and lower cost of GPS-based TSP strategy, compared with traditional TSP strategy were considered, GPS-based TSP strategy seemed preferable for existing TSP system upgrades and new TSP system implementations. The tests of CTSP and CTSP2 strategies showed benefits of function extensions to GPS-based TSP. With TSP constraints, which are applied to the buses with a

higher occupancy and in need of a schedule catch-up, the transit system still experienced considerable delay reductions and travel time savings compared with the base scenario. At the same time, CTSP2 strategy had minimal negative impacts on side-street traffic compared with other TSP strategies.

As the models were built according to the specific situations of the selected transit route in Salt Lake County, the simulation results and the analysis made on the basis of these results cannot fully cover the range of situations on transit routes in other parts of the country. However, the comparisons of scenarios can provide insights to the differences in effectiveness and impacts of alternative TSP strategies.

Even though GPS-based TSP strategy has multiple advantages over traditional systems, it can be inaccurate in densely built environments because of the urban-canyon effect. For this reason, geographical features and technology capabilities should be fully considered when GPS-based systems are being implemented and operated. Research seeking to identify potential cost-effective solutions for the GPS urban-canyon problem is ongoing, and various alternatives are likely to become available in the future.

On the basis of the findings of this study, future studies will focus on evaluating adaptive TSP strategies, which involve communications between GPS-based TSP systems and other intelligent traffic operation systems to see whether it can more effectively use signal priority and maintain the minimum impacts to traffic operations at the corridor and network levels.

6.2 DT Modeling for TVM Effectiveness Analysis

DT has significant impacts on transit reliability and operational efficiency. A practical modeling approach is needed to objectively and quantitatively determine the factors that contribute most to DT and can be supported with the availability of APC data in the majority of transit systems. Greater insights can be gained through more robust datasets to reveal the separate impacts of fare payment structure, which empirically constitutes the major influence on DT. Although APC/AFC datasets offer ample amounts of information for transit performance analysis, the data fail to reflect the fare transactions that do not have electronic footage, which still account for a large portion of the fare payment structure in most transit systems. It thus imposes challenges in accurately estimating their impact on DT and hinders transit efficiency analysis for service optimization and performance assessment.

The analysis and proposed modeling approach showed that the gap in fare payment structure estimation might be remedied by treating the DT observations as an optimization problem. GA was applied to the APC dataset to classify the DT observations into behavior-controlled classes: BC, AC, and atypical scenarios. A combined modeling approach of GA and regression analysis was able to identify the fare payment structure (split of different payment types at the station level) and subsequently quantify their impact on DT. The modeling approach was implemented using data gathered along 35M BRT operated by UTA in Salt Lake City, serving as the pioneer BRT project with several other BRT lines being planned in the near future. The route allows for several fare payment options, and inspired this research given recent inquiries regarding the possible mass deployment of TVMs at every BRT station and their likely effectiveness in improving transit operational efficiency.

The final model for DT prediction showed an excellent goodness-of-fit with an adjusted R-squared of 0.90. Validity testing indicated possible estimation bias introduced by the GA estimation of some portions of the fare payment structure was relatively small. The model demonstrated the advantage of off-board fare collection over on-board fare collection, with average boarding times of 5.2, 1.8, and 6.9 seconds estimated for passengers using smart cards, prepaid passes, and on-board cash payments, respectively. Built environment and stop design also had impacts on DT, as stations located on the median of the roadway were found to have shorter DT, and the ones located near shopping malls or hospitals tended to

have longer DT. The modeling approach is transferable to any transit routes or systems with access to the APC/AFC database and can help reveal why DT under certain conditions (time-of-day, station, passenger population, etc.) is likely to persist. The result of the model should not be the final word on the matter; rather it motivates the need for a next logical step: to provide guidelines and further analysis that is policy driven, such as fare evasion estimation, TVM cost-benefit analysis, and instructional guidance to facilitate smooth boarding/alighting process, all in an effort to improve transit efficiency and reduce DT variation. The results can be potentially useful to future BRT projects. Additional analysis on more specific impacts of the built environment is also needed, and will require data that represent the range of common characteristics for these variables.

REFERENCES

- Aashtiani, H., and H. Iravani. "Application of Dwell Time Functions in Transit Assignment Model." In *Transportation Research Record: Journal of the Transportation Research Board*, No. 1817, Transportation Research Board of the National Academies, Washington, D.C., 2002, pp. 88–92.
- Bertini, R. L., and A. M. El-Geneidy. "Modeling Transit Trip Time Using Archived Bus Dispatch System Data." *Journal of Transportation Engineering*, Vol. 130, No. 1, 2004, pp. 56–67.
- Bloomberg, L., and J. Dale. "Comparison of VISSIM and CORSIM Traffic Simulation Models on a Congested Network." In *Transportation Research Record: Journal of the Transportation Research Board*, No. 1727, 2000, pp. 52–60.
- Chen, X., L. Yu, L. Zhu, L. Yu, and J. Guo. "Microscopic Simulation Approach to Effectiveness Analysis of Transit Signal Priority for Bus Rapid Transit: A Case Study in Beijing." In *Transportation Research Record: Journal of the Transportation Research Board*, No. 2072, 2008.
- Chang, G. L. Review of Transit Signal Priority (TSP) Policies and Strategies. Presented at Traffic Safety and Operation Lab, University of Maryland, Aug. 2012.
- Dueker, K. J., T. J. Kimpel, and J. G. Strathman. "Determinants of Bus Dwell Time." *Journal of Public Transportation*, Vol. 7, No. 1, 2004, pp. 21–39.
- Dale, J. J., T. Bauer, R. J. Atherley, and L. Madsen. A Transit Signal Priority Impact Assessment Methodology: Greater Reliance on Simulation. Presented at 78th Annual Meeting of the Transportation Research Board, Washington, D.C., 1999.
- Dion, F., H. Rakha, and Y. Zhang. "Evaluation of Potential Transit Signal Priority Benefits Along a Fixed-Time Signalized Arterial." *Journal of Transportation Engineering*, Vol. 130, No. 3, 2004, pp. 294–303.
- Dion, F., and H. Rakha. Integration of Transit Signal Priority Within Adaptive Traffic Signal Control Systems. Presented at 84th Annual Meeting of the Transportation Research Board, Washington, D.C., 2005.
- Feder, R. C. *The Effect of Bus Stop Spacing and Location on Travel Time*. Report No. CMUTRI-TP-73-14. Transportation Research Institute, Carnegie Mellon University, Pittsburgh, Pa., 1973.
- Fletcher, G., and A. El-Geneidy. "Effects of Fare Payment Types and Crowding on Dwell Time: Fine-Grained Analysis." In *Transportation Research Record: Journal of the Transportation Research Board*, No. 2351, Transportation Research Board of the National Academies, Washington, D.C., 2013, pp. 124–132.
- Ghanim, M. S., G. Abu-Lebdeh, and K. Ahmed. Microscopic Simulation Study of Transit Signal Priority Implementation Along an Arterial Corridor. Presented at 5th International Conference on Modeling, Simulation and Applied Optimization, IEEE, Hammamet, Tunisia, April 2013.
- Guenther, R. P., and K. C. Sinha. "Modeling Bus Delays Due to Passenger Boardings and Alightings." In *Transportation Research Record 915*, TRB, National Research Council, Washington, D.C., 1983, pp. 7–13.

- Guenthner, R. P., and K. Hamat. "Transit Dwell Time Under Complex Fare Structure." *Journal of Transportation Engineering*, Vol. 114, 1988, pp. 279–367.
- Hausman, J. A. Specification Tests in Econometrics. *Econometrica*, Vol. 46, 1978, pp. 1251–1271.
- Innovative Transportation Concepts, Inc. *TSP State-of-the-Practice, Regional Transit Signal Priority Location Study, Phase II: Model Simulation*. Regional Transportation Authority, Chicago, Ill., Aug. 2001.
- Kraft, W. H., and T. F. Bergen. "Evaluation of Passenger Service Times for Street Transit Systems." In *Transportation Research Record 505*, TRB, National Research Council, Washington, D.C., 1974, pp. 13–20.
- Levine, J. C., and G. W. Torng. "Dwell-Time Effects of Low-Floor Bus Design." *Journal of Transportation Engineering*, Vol. 120, 1994, pp. 914–929.
- Levinson, H. S. "Analyzing Transit Travel Time Performance." In *Transportation Research Record 915*, TRB, National Research Council, Washington, D.C., 1983, pp. 1–6.
- Li, Y., P. Koonce, M. Li, K. Zhou, Y. Li, S. Beaird, W.-B. Zhang, L. Hegen, K. Hu, A. Skabardonis, and Z. S. Sun, *Transit Signal Priority Research Tools*. UCB-ITS-PRR-2008-4. California PATH, Richmond, April 2008.
- Liao, C.-F., and G. A. Davis. *Field Testing and Evaluation of a Wireless-Based Transit Signal Priority System*. CTS 11-25. Center for Transportation Studies, University of Minnesota, Minneapolis, Oct. 2011.
- Li, M., K. Zhou, W.-B. Zhang, Y. Li, G. Wu, and F. Bu. *Field Operational Tests of Conditional Transit Signal Priority Systems*. UCB-ITS-PRR-2010-35, California PATH, Richmond, June 2010.
- Lin, T., and N. H. M. Wilson. "Dwell Time Relationships for Light Rail Systems." In *Transportation Research Record 1361*, TRB, National Research Council, Washington, D.C., 1992, pp. 287–295.
- Martin, A., H. Ross, J. McGlashan, K. Sharma, and T. Hiles. *Transit Signal Priority: A Look at the Impacts on High-Volume Coordinated Cross-Streets*. Presented at ITE 2010 Annual Meeting, Vancouver, British Columbia, Canada, August, 2010.
- Milkovits, M. N. "Modeling the Factors Affecting Bus Stop Dwell Time: Use of Automatic Passenger Counting, Automatic Fare Counting, and Automatic Vehicle Location Data." In *Transportation Research Record: Journal of the Transportation Research Board*, No. 2072, Transportation Research Board of the National Academies, Washington, D.C., 2008, pp. 125–130.
- Park, B., and J. Hu. *Transit Signal Priority with Connected Vehicle Technology*. UVA-2012-04. University of Virginia, Charlottesville, Jan. 2014.
- Rajbhandari, R., S. I. Chien, and J. R. Daniel. "Estimation of Bus Dwell Times with Automatic Passenger Counter Information." In *Transportation Research Record: Journal of the Transportation Research Board*, No. 1841, Transportation Research Board of the National Academies, Washington, D.C., 2003, pp. 120–127.

- Stewart, C., and A. El-Geneidy. "All Aboard at All Doors: Route Selection and Running-Time Savings Estimation for Multiscenario All-Door Bus Boarding." In *Transportation Research Record: Journal of the Transportation Research Board*, No. 2418, Transportation Research Board of the National Academies, Washington, D.C., 2014, pp. 39–48.
- Smith, H. R., B. Hemily, and M. Ivanovic. *Transit Signal Priority (TSP): A Planning and Implementation Handbook*, ITS America, Washington, D.C., May 2005.
- Sun, L., A. Tirachini, K. Axhausen, A. Erath, and D. Leeb. "Models of Bus Boarding and Alighting Dynamics." *Transportation Research Part A*, Vol. 69, 2014, pp. 447–460.
- TCRP Report 118: Bus Rapid Transit Practitioner's Guide*. Transportation Research Board of the National Academies, Washington, D.C., 2007.
- TCRP Report 165: Transit Capacity and Quality of Service Manual*. 3rd ed. Transportation Research Board of the National Academies, Washington, D.C., 2003.
- Tirachini, A. "Estimation of Travel Time and the Benefits of Upgrading the Fare Payment Technology in Urban Bus Services." *Transportation Research Part C*, Vol. 30, 2013, pp. 239–256.
- Tirachini, A. "Bus Dwell Time: The Effect of Different Fare Collection Systems, Bus Floor Level and Age of Passengers." *Transportmetrica A, Transport Science*, Vol. 9, 2013, pp. 28–49.
- Utah Department of Transportation. *AADT Map*.
<http://www.udot.utah.gov/main/uconowner.gf?n=1439512064832147>.
- Utah Transit Authority, 2014. UTA bus rapid transit design criteria.
- Weesie, J. "Seemingly Unrelated Estimation and the Cluster-Adjusted Sandwich Estimator." *Stata Technical Bulletin*, Vol. 52, pp. 34–47.
- Zlatkovic, M., A. Stevanovic, and R. M. Z. Reza. Effects of Queue Jumpers and Transit Signal Priority on Bus Rapid Transit. Presented at 92nd Annual Meeting of the Transportation Research Board, Washington, D.C., 2013.